

## Influence of Cross-Sectional Geometry on Mixing in a T-Shaped Micro-Junction

Alessandro Mariotti, Michele Lanzetta, Gino Dini, Andrea Rossi, Elisabetta Brunazzi, Roberto Mauri, Chiara Galletti\*

Dipartimento di Ingegneria Civile e Industriale, Università di Pisa, Largo Lucio Lazzarino 2, 56122 Pisa, Italy.  
 chiara.galletti@unipi.it

Microfluidics is gaining increasing interest in the field of chemical engineering, as miniaturization may lead to a significant intensification of chemical processes. Since the flow is laminar, achieving a good mixing of reactants is one of the main challenges. The simplest geometry is constituted by a T-shaped mixer in which the two inlets join perpendicularly the mixing channel. The inlet cross section is usually square while the mixing channel cross-section is a rectangle as straight walls facilitate experimental and modelling analysis. The present work, on the contrary, is aimed at investigating through Computational Fluid Dynamics the effect of a cross-section with lateral inclined walls, to emulate a microfabrication technology based on laser machining. The presence of inclined walls is found to hamper mixing at high Reynolds numbers as the flow is unable to break the mirror symmetry and thus to undergo the engulfment regime. However, at low Reynolds numbers the mixing is improved because the vortex regime presents a lower degree of symmetry with respect to that of T-mixers with straight walls.

### 1. Introduction

Micro-reactor technology is gaining increasing interest for a wide range of applications, including the intensification of chemical reactions for the pharmaceutical and fine chemical industries as well as the production of micro-particles. The main reason for preferring micro-reactors to conventional batch reactors is the excellent control over operating conditions that micro-devices offer due to the laminar regime and enhanced heat transfer. This, for instance, makes possible to handle highly exothermic or dangerous reactions without the need of any dilution that would be required in conventional batch stirred vessels.

The increased interest in this field is also demonstrated by the large number of polymer microfabrication technologies established over the recent years and divided in two categories, i.e. additive and subtractive ones. The additive technology represents a very promising approach, but it is affected by some critical issues related, in particular, to the quite low achievable resolution. The subtractive technology, such as chemical etching process or traditional milling, allows to obtain more accurate micro-channels. In this last category, laser machining is emerging as an efficient way of fabrication, not only for the speed of the process itself, but also for the high flexibility in micro-reactor design and for an easy control and repeatability of the cross-section geometry. One of the main challenges in micro-devices is to achieve a good mixing of reactants. This is also fundamental in micro-particle formation processes as those based on the solvent/anti-solvent method. The main problem is that the flow field is laminar; hence mixing should be improved by means of proper mixing enhancement techniques, that can be either active or passive. Active methods involve external energy sources (i.e. ultrasound, pressure disturbance, etc.), while passive methods are based on a clever design of the mixer aimed at breaking the flow symmetries. To this purpose, a large variety of geometries has been proposed so far, always keeping in mind that the geometry should be also simple to fabricate (Roudgar et al., 2012). The simplest mixer is a T-shaped one, in which the inlets join the mixing channel through T-shaped branches. Despite this very simple geometry, the flow field is surprisingly complex, even presenting flow instabilities that may improve or dampen mixing (Mariotti et al., 2018). For instance, when the two inlets of a T-mixer with square inlet cross-sections are fed with water at the same flow rates, different flow regimes may

Paper Received: 16 March 2018; Revised: 12 August 2018; Accepted: 10 January 2019

Please cite this article as: Mariotti A., Lanzetta M., Dini G., Rossi A., Brunazzi E., Mauri R., Galletti C., 2019, Influence of Cross-sectional Geometry on Mixing in a T-shaped Micro-junction, Chemical Engineering Transactions, 74, 955-960 DOI:10.3303/CET1974160

be present, depending of the Reynolds number,  $Re$ . In particular, it was shown that the inlet streams remain separated up to a critical  $Re$ , corresponding to the transition from a vortex flow regime, which is characterized by symmetric features with respect to the mixer mid-plane, to an engulfment flow regime, which is able to provide a large increase of the degree of mixing thanks to its large asymmetry. Then, by further increasing  $Re$ , the flow becomes unsteady and time-periodic, still preserving asymmetric features, so that these instabilities strongly improve mixing. However, and unexpectedly, with a further increase of  $Re$ , the flow undergoes a rapid transition leading to a time-periodic motion with a large degree of symmetry, which strongly hampers the mixing of the inlet streams. Finally, by an additional increase of the flow rate, the flow becomes chaotic.

The aforementioned results have been observed both experimentally and numerically, thus determining the effects of the mixing channel aspect ratio (Andreussi et al., 2015), the inclination angle of the inlet channels (Mariotti et al., 2019) or the fluid properties (Orsi et al., 2013; Galletti et al., 2015; Galletti et al., 2017). Most of the past investigations have assumed that both inlet and mixing channel cross-sections are either square or rectangular, as straight walls facilitate experimental and modelling analysis. The present work, on the contrary, is aimed at investigating the effect of a cross-section with lateral inclined walls, easy to be obtained on a polymethylmetacrilate (PMMA) substrate by using a CO<sub>2</sub> laser subtraction process, as demonstrated in Romoli et al. (2007, 2011) where a theoretical model for the prediction of the cross-section geometry as a function of the process parameters was also proposed. The extension to harder materials (ceramics) for improved durability and contamination resistance is dealt in Dalle Mura et al. (2018).

## 2. Fabrication

The fabrication procedure to obtain the cross-section is illustrated in Figure 1. It mainly consists of two phases: a cutting phase (Figure 1b), where the PMMA layer is cut by the laser beam (vaporization affects both PMMA layer and sacrificial layer) and then a bonding phase (Figure 1c), using a combination of pressure and heating in order to set the layer temperature just over the glass transition value. Figure 2 shows the cross-section obtained by one pass of laser beam and the corresponding trapezoidal cross-section adopted in the present study. The process parameters can be set using the model of Romoli et al. (2007, 2011). Table 1 reports the values of width  $W$  and depth  $D$  obtained according to the laser energy density; the final channel height  $h$  is obviously less than  $D$  and corresponds to the thickness of the central layer at the end of the bonding phase. Combinations of CO<sub>2</sub> laser spot sizes and scanning speeds are able to produce walls with different inclinations and aspect ratios, as an approximation of Gaussian like and elliptical profiles obtained respectively on PMMA and zirconia. As for the mass manufacturing of micro-reactors, experiments at 20 W have shown a material removal rate respectively of 5 and 7.8 mm<sup>3</sup>/s, with a linear speed of 20 mm/s.

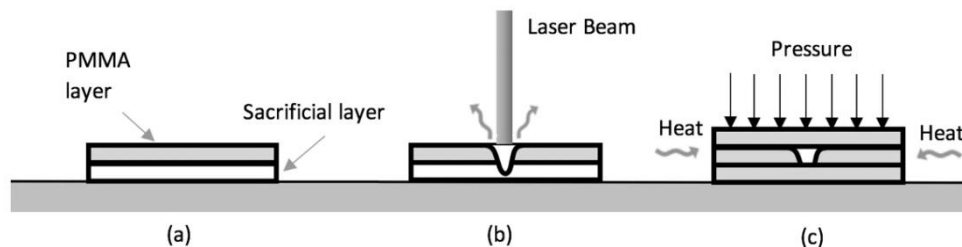


Figure 1: Micro-channel fabrication: a) starting configuration; b) laser cutting phase; c) thermal bonding phase.

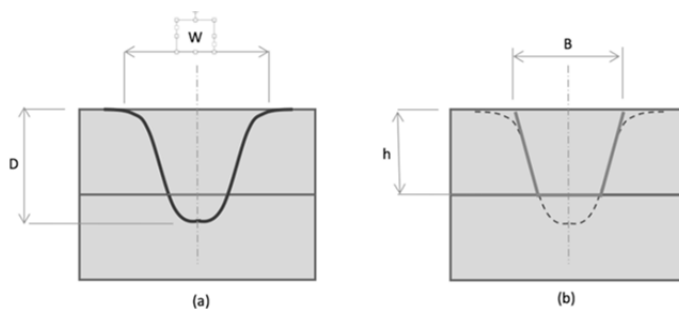


Figure 2: a) Micro-channel cross-section obtained with one pass of laser beam; b) trapezoidal section analysed in the present case.

Table 1: Mean values of width  $W$  and depth  $D$  obtained on PMMA layer using a  $CO_2$  laser.

$\varepsilon$ [J/m]	$W$ [ $\mu\text{m}$ ]	$D$ [ $\mu\text{m}$ ]
200	410	250
250	440	300
300	470	360
350	490	410
400	500	500

### 3. T-mixer geometry and operating conditions

The investigated mixer has a T-shape with a trapezoidal cross-section and is shown in Figure 3 along with its main dimensions. The mixer was built in order to have the same inclination ( $25^\circ$ ) of the inlet and mixing channel walls, and to have a mixing channel cross-section area which is double the inlet ones (the two inlet channels are identical). In this manner, no acceleration effects are present, i.e. the mean fluid velocity in the two inlets,  $U$ , is the same as the mean fluid velocity in the outlet. The hydraulic diameter of the inlet channels was chosen to be  $d_{h,i}=100\ \mu\text{m}$ ; hence the hydraulic diameter of the mixing channel is  $d_h=141\ \mu\text{m}$ . The length of the inlet channels is  $L_i = 20d_{h,i}$  in order to allow the flow to be fully developed at the confluence of the two inlet streams, while the length of the mixing channel is  $L = 30d_h$ . The T-mixer is fed with water at ambient conditions and equal flow rates from the two inlets. The Reynolds number is defined using the average velocity and the hydraulic diameter of the mixing channel, i.e.,  $Re = d_h U / \nu =$ , where  $\nu$  is the kinematic viscosity of the fluid.

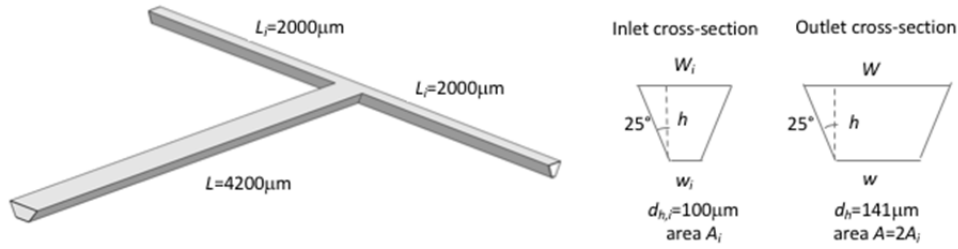


Figure 3: T-mixer geometry.

### 4. Numerical model

Steady-state Navier-Stokes equations for an incompressible fluid were solved with the code ANSYS® Fluent v18. The non-dimensional form of the equation is:

$$\nabla \cdot \mathbf{u} = 0 \quad (1)$$

$$\mathbf{u} \cdot \nabla \mathbf{u} = -\nabla P + \frac{1}{Re} \nabla^2 \mathbf{u} \quad (2)$$

where length, velocities and time are normalized with the mixing channel hydraulic diameter  $d_h$  and the inlet bulk velocity  $U$ .  $P$  is the modified non-dimensional pressure. These equations are coupled with a transport equation for a conservative scalar representing a dye, to distinguish between the two inlet water streams:

$$\mathbf{u} \cdot \nabla \phi = \frac{1}{Pe} \nabla^2 \phi \quad (3)$$

Here  $\phi$  is the dye mass fraction and  $Pe = Ud_h/D$  is the Peclet number, where  $D$  is the dye molecular diffusivity. Since liquids present a very large Schmidt number, i.e.  $Sc = \nu/D = \mathcal{O}(10^3 - 10^4)$  and in the present case  $Re = \mathcal{O}(10^2)$ , the resulting Peclet number  $Pe = ReSc = \mathcal{O}(10^5 - 10^6)$  (Galletti et al., 2019). A block structured grid was generated using the ICFM software by ANSYS®. The grid consisted of 700k elements and resulted from a grid independency study, carried out using a number of cells from 200k to 1M. Uniform velocities were set at the two inlets; this boundary condition does not affect results as the inlet channels are long enough to allow the full development of the flow (Galletti et al., 2012). No slip conditions were set at the walls, while a pressure condition was set at the outlet. A second order discretization scheme was adopted using the SIMPLE algorithm to treat the pressure-velocity coupling. The numerical approach has been successfully validated against experimental flow visualizations and benchmarked also with other numerical

models (i.e. using spectral element codes) for a T-mixer with square inlet cross-sections (Mariotti et al., 2018; Galletti et al., 2019).

## 5. Results

The dye distributions obtained at different Reynolds numbers in the mixing channel cross-sections at a distance  $y=10d_h$  from the confluence region are shown in Figure 4 and compared with those obtained in a T-mixer with square inlet cross-sections (i.e. not inclined walls, see Mariotti et al., 2018). At  $Re = 100$  the flow in the mixer with square inlet cross-sections is segregated, with almost no degree of mixing (Figure 4d). The T-mixer with trapezoidal cross-sections shows also a segregated flow, albeit some degree of mixing can be observed (Figure 4a). By increasing the flow rate, the flow in the T-mixer with square inlet cross-sections undergoes a transition to the engulfment regime, leading to a sudden increase of the degree of mixing (see Figure 4e at  $Re = 200$ ). Conversely the flow in the T-mixer with trapezoidal cross-sections appears to remain segregated, although presenting some mixing (see Figure 4b at  $Re = 200$  and Figure 4c at  $Re = 300$ ). The corresponding in-plane velocity vectors and normal vorticity in the same mixing channel cross-section are shown in Figure 5. At  $Re = 100$  for the T-mixer with square inlet cross-sections, they indicate the presence of two pairs of two weak counter-rotating vortices of equal strengths (see Figure 5d), thus exhibiting a double mirror symmetry. Instead, the flow in the mixer with trapezoidal cross-sections presents only two stronger counter-rotating vortices with a single mirror symmetry. Further increasing  $Re$ , the flow in such mixer is unable to break this mirror symmetry with respect to the channel mid-plane (see Figure 5b at  $Re=200$  and Figure 5c at  $Re=300$ ). Conversely, the flow at  $Re=200$  in the mixer with square inlet cross-sections clearly presents a breaking of the flow symmetry (Figure 5e), resulting in two strong co-rotating vortices.

A better understanding of the mixing process can be achieved through the visualization of vortical structures in the mixer as reported in Figure 6. These vortical structures are identified through the  $\lambda_2$ -criterion (Jeong and Hussain, 1995), which defines a vortex as a connected fluid region where the second largest eigenvalue of the symmetric tensor  $L = S \cdot S + A \cdot A$  is negative. Here,  $S$  and  $A$  are the symmetric and anti-symmetric parts of the velocity gradient, i.e. the strain rate and vorticity tensors, respectively.

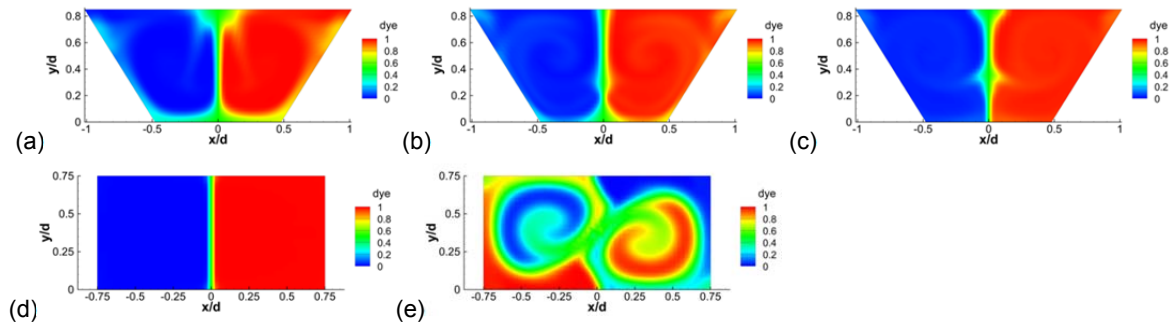


Figure 4: Dye distribution (red=dye, blue=no dye) in the mixing channel cross-section at  $y/d_h=10$  obtained for the T-mixers with (a,b,c) trapezoidal and (d,e) square inlet cross-sections at: (a,d)  $Re=100$ ; (b,e)  $Re=200$ ; (c)  $Re=300$ .

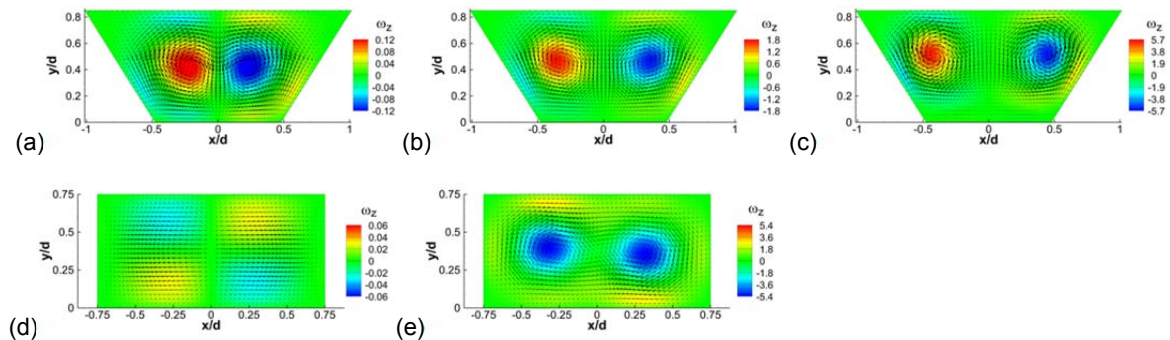


Figure 5: In-plane velocity vectors and normal vorticity distribution ( $1/s$ ) in the mixing channel cross-section at  $y/d_h=10$  obtained for the T-mixers with (a,b,c) trapezoidal and (d,e) square inlet cross-sections at: (a,d)  $Re=100$ ; (b,e)  $Re=200$ ; (c)  $Re=300$ .

Figure 6a shows 3 views (including front and top views) of the vortical structures in the T-mixer with trapezoidal cross-sections at  $Re = 100$ , while in Figure 6d the vortical structures in the T-mixer with square inlets are reported for sake of comparison. For more details about the flow behavior in the T-mixer with square inlets, please see Mariotti et al. (2018). The flow at  $Re = 100$  in this latter mixer is characterized by a double pair of counter-rotating vortices, leading to four legs of equal strength in the mixing channel (vortex regime). Instead, the T-mixer with trapezoidal cross-sections presents two strong and two weak legs, still preserving the mirror symmetry with respect to the channel mid-plane. Only the two strongest legs survive in the mixing channel, leading to the normal vorticity distribution of Figure 5a at  $y = 10d_h$ . At  $Re = 200$  the T-mixer with square inlet cross-sections shows a tilting of the vortical structures at the top the mixer, which leads to the formation of two strong and two weak co-rotating legs in the mixing channel, with only the strongest legs surviving in the channel. The mirror symmetry is lost (see Figure 6e). This is the engulfment regime and is characterized by a strong increase of mixing. Instead, the T-mixer with trapezoidal cross-sections is unable to break the mirror symmetry (Figure 6b), so that the mixing process is hampered. A further increase of the Reynolds number up to  $Re = 300$  leads to some swirling of the strongest legs, and thus to a minor increase of the degree of mixing. Please note that in Figures 4-6 the case  $Re = 300$  is not reported for the T-mixer with square inlet cross-sections as for such Reynolds number the flow is unsteady and time-periodic (Salveti et al., 2018). Instead, for the T-mixer with trapezoidal cross-sections the flow becomes unsteady at approximately  $Re = 325$ .

The degree of mixing  $\delta_m$  is estimated for the mixer with inclined walls using the cup-mixing average (Galletti et al. 2015) and is compared to that of a T-mixer with square inlet cross-sections in Figure 7. The latter T-mixer shows a sudden increase of  $\delta_m$  at the onset of the engulfment regime, which, occurs at approximately  $Re = 145$ . The mixer with inclined walls, instead, shows a gradual increase of the degree of mixing. At  $Re = 50$ , the degree of mixing is of about  $\delta_m = 8\%$ , thus significant larger than that of the T-mixer with square inlet cross-sections (approximately  $\delta_m = 1.5\%$ ). Subsequently the degree of mixing in case of inclined walls slowly increases due to the swirling of the vertical legs in the mixing channel, but remains considerably smaller than the one achieved for the T-mixer with square inlet cross-sections in the engulfment regime.

## 6. Conclusions

The mixing process in a T-shaped mixer with inclined side walls has been investigated through CFD, in order to emulate laser machining, which represents a promising subtractive microfabrication technology. Inclined side walls hamper the bifurcation leading to the engulfment regime, deeply analysed in T-mixers with straight walls.

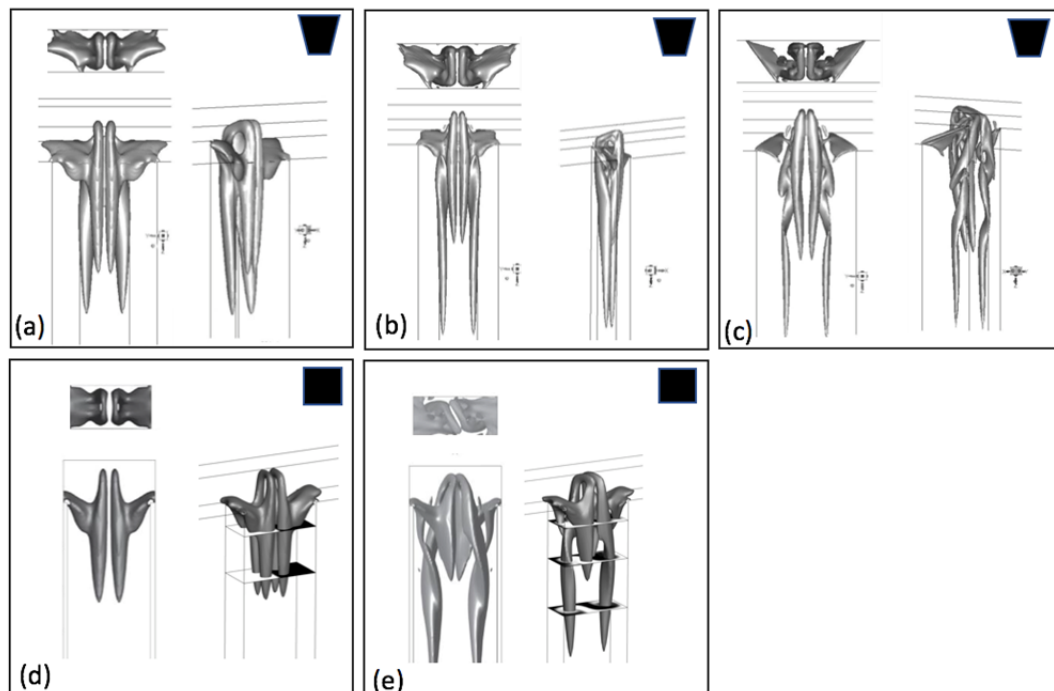


Figure 6: Vortical structures as identified by the  $\lambda_2$ -criterion for different Reynolds number: (a,d)  $Re = 100$ ; (b,e)  $Re=200$ ; (c)  $Re=300$ . T-mixer with (a,b,c) trapezoidal and (d,e) square inlet cross-sections.

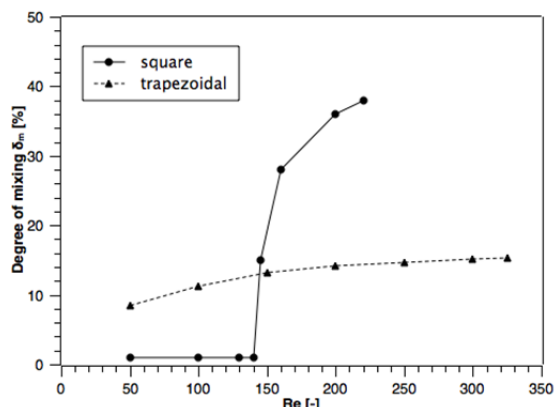


Figure 7: Degree of mixing as a function of the Reynolds number.

However, at low Reynolds numbers the performance is superior because the vortical structures in the mixing channels have different strengths and thus exhibit a low degree of symmetry. Future work is required to evaluate the sensitivity of the degree of mixing on the morphological adherence (e.g. edge sharpness, dimensions).

### Acknowledgments

This work was supported by University of Pisa, Italy, through the “Progetti di Ricerca di Ateneo PRA 2017–2018” funding program. The authors wish to thank Eleonora Landi and Alberto Rossi for their numerical simulations.

### References

- Andreussi T., Galletti C., Mauri R., Camarri S., Salvetti M.V., 2015, Flow regimes in T-shaped micro-mixers *Computers and Chemical Engineering*, 76, 150-159.
- Dalle Mura M., Dini G., Lanzetta M., Rossi A., 2018. An Experimental Analysis of Laser Machining for Dental Implants. *Procedia CIRP*, 67, 356-361.
- Galletti C., Roudgar M., Brunazzi E., Mauri R., 2012, Effect of inlet conditions on the engulfment pattern in a T-shaped micro-mixer, *Chemical Engineering Journal*, 185-186, 300-313.
- Galletti C., Arcolini G., Brunazzi E., Mauri R., 2015, Mixing of binary fluids with composition-dependent viscosity in a T-shaped micro-device, *Chemical Engineering Science*, 123, 300-310.
- Galletti C., Brunazzi E., Mauri R., 2017, Unsteady mixing of binary liquid mixtures with composition-dependent viscosity, *Chemical Engineering Science*, 164, 333-343.
- Galletti C., Mariotti A., Siconolfi L., Mauri R., Brunazzi E., 2019, Numerical investigation of flow regimes in T-shaped micromixers: Benchmark between finite volume and spectral element methods, *Canadian Journal of Chemical Engineering*, 97, 528-541.
- Jeong J., Hussain F., 1995, On the identification of a vortex, *Journal of Fluid Mechanics* 285, 69–94.
- Orsi G., Galletti C., Brunazzi E., Mauri R., 2013, Mixing of two miscible liquids in T-shaped microdevices, *Chemical Engineering Transactions*, 32, 1471-1476.
- Roudgar M., Brunazzi E., Galletti C., Mauri R., 2012, Numerical Study of Split T-Micromixers, *Chemical Engineering and Technology*, 35, 1291-1299.
- Mariotti A., Galletti C., Mauri R., Salvetti M.V., Brunazzi E., 2018, Steady and unsteady regimes in a T-shaped micro-mixer: synergic experimental and numerical investigation, *Chemical Engineering Journal*, 341, 414-431.
- Mariotti A., Galletti C., Brunazzi E., Salvetti M.V., 2019, Steady flow regimes and mixing performance in arrow-shaped micro-mixers, *Physical Review Fluids*, 4, 034201.
- Romoli L., Tantussi G., Dini G., 2011, Experimental approach to the laser machining of PMMA substrates for the fabrication of microfluidic device, *Optics and Lasers in Engineering*, 49, 419-427.
- Romoli L., Tantussi G., Dini G., 2007, Layered Laser Vaporization of PMMA Manufacturing 3D Mould Cavities, *Annals of the CIRP*, 56, 209-212.
- Salvetti M.V., Mariotti A., Galletti C., Brunazzi E., 2018, Experimental and numerical analyses of unsteady flow regimes and mixing in a micro T-mixer, In *Proceedings of the FEDSM 2018*, American Society of Mechanical Engineers, Fluids Engineering Division, 3, 141102.